Design and Simulation of a Waveguide Division De-multiplexer (DWDM) for Communication Application

Yadollah Shahamat[1], Mohamad Vahedi[1*]
1- Department of Physics, Iran University of Science and Technology, Tehran, Iran.
Email: mehdyshahamat@yahoo.com
Email: mvahed@iust.ac.ir (Corresponding author)

Received: July 2018 Revised: August 2018 Accepted: October 2018

ABSTRACT:
In this paper, we design and simulate a novel wavelength division demultiplexer (WDDM) based on photonic crystal (PC), with high efficiency and without using either special materials or complexities in fabrication process. The photonic crystal consists of a square lattice of Chalcogenide glass with n=2.597 embedded in the air in two dimensions. The structure involves three cavities around the boundary of a waveguide inside the PC with certain distance from each other for wavelength selection. For obtaining resonant frequency of the cavities, two-dimensional Finite-Difference-Time-Domain (FDTD) is used. Through simulations, characteristic resonant wavelengths of the cavities are obtained for different radii of the coupling rods (R_1) and the inner rod of the cavity (R_2). Our simulations indicate that appropriate selections of R_1 and R_2 for efficiently separating wavelengths 1.53, 1.54 and 1.56 µm are 128.126 nm and 0, 120.438 nm and 0, 116.594nm and 38.43nm, respectively. Equipped with these design parameters a WDDM is proposed.

KEYWORDS: Wavelength Division Demultiplexer (WDDM), Photonic Crystal, Finite-Difference-Time-Domain (FDTD), Resonant Wavelengths.

1. INTRODUCTION

With the advent of multi-media communications, the traffic of the telecommunication network increased and the requirement to provide a new network with high capacity was sensed. Due to the enormous advantages of optical systems over electrical systems, they were introduced as the best candidate for telecommunication network. Optical Wavelength Division Demultiplexing (WDDM) devices enables us to distinguish between hundreds or even thousands of different wavelengths of a light signal in an optical fiber.

One of the best candidates for employing optical WDDM devices are photonic crystals (PCs), because the principle of operation of PCs are mainly based on the refractive index difference and their specific geometry. In a simple definition, PCs are a periodic array of rods or holes in a background medium in one, two or three dimensions. The lattice constant in photonic crystals demonstrate the minimum length that crystal repeats its structure. An important consequence of this periodicity is a feature that is called photonic band gap (PBG). This means that light waves could not propagate through the photonic crystals for frequency ranges located in the PBG [1, 2]. Due to such property and other properties of PCs, optical photonic crystal waveguides (PCWs) are used widely in optical network systems. By constructing a waveguide in a perfect photonic crystal, the symmetry of the crystal is broken and PC permits propagating of light in the waveguide path [3, 4].

It has been shown that by introduction of a point defect inside a PCW, a sharp resonant state inside the crystal in the vicinity of the defect is created [5-12]. Chen-Yang Liu *et al* proposed a tunable PC channel drop filter [13]. They placed some cavities containing liquid crystals in the PCW and therefore succeeded to build a tunable filter. The drawback of their design is that liquids have a high optical absorption coefficient, which causes high percentage absorption of the light energy and therefore the device quickly loses its performance.

In this paper, we present a different design for WDDM based on PCW for separating wavelengths of the input light with high functionality and efficiency. The device is made of Chalcogenide glass (As-S-Se) rods in the air background. The structure consists of special cavities, made of rods with different radii and refractive indices from PC structure, that select special wavelengths. Chalcogenide are used because they could be formed over a wide range of compositions and their refractive index is typically between 2.4 and 3 that is high enough to obtain big PBGs. In addition, these glasses do not have high absorption coefficient. They are also loss-less around infrared wavelengths and have a low two-photon absorption cross-section compared to other materials commonly used for PC fabrication such as Si. In the first step, we find the best (widest) band-gap for our photonic crystal by changing the ratio of the radius of the rods to the lattice constant. Next, we present a simple T-shaped waveguide that has a special cavity in its path. Our results show that by modifying the radius of the rod inside the cavity (R_2) and rods up and down the cavity (R_1), resonant frequency of the cavity will change. At the end of the paper, we use these results to design a demultiplexer for separating three wavelengths. In each step, the resonant frequency of the cavities is obtained by lunching a pulse at input port and then taking the Fourier transform of the time-dependent field at the detector position.

2. NUMERICAL MODEL

To study the electromagnetic wave behavior, numerical solutions are used. There are several methods for PC analysis such as Plane Wave Expansion (PWE) and Finite Difference Time Domain (FDTD) [14, 15]. PWE method is usually employed to obtain photonic crystals band gap (PBG) and FDTD method is employed to obtain frequency response of the structure. The advantage of PWE methods is high computing speed. However, the problem is its limitation to application for calculating the stationary states. The FDTD is an accurate method for studying and analyzing electromagnetic problems that has dispersive and nonlinear behaviors. In this paper, we calculate the band gap structure by using PWE method and use FDTD method for calculating resonant wavelength of the cavity. We use perfectly matched layer boundary condition (PML) [16] with 500 nm width that is placed on the structure boundary to reduce the back reflection from the end of the PBG lattice during computation.

3. WDDM DESIGN

Fig 1 illustrates a schematically cross-sectional view of the PhC lattice. The shaded region in Fig. 1 illustrates the lattice unit cell that represents the computational domain whose borders are terminated by PBC

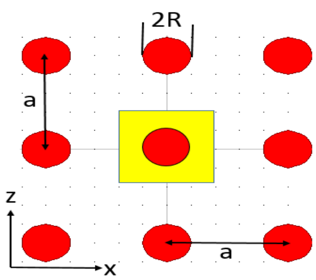

Fig. 1. A schematic cross-sectional view of the 2D PhC structure with a square lattice.

In the first step, the gap map diagram in terms of parameter (r/a) is calculated for achieving maximum value of the band-gap in Transverse Electric (TE) mode (electric field is parallel to the rod axis). Fig. 2 shows gap map diagram where the horizontal axis represents the parameter (r/a) and the z axis shows the normalized frequency "ωa/2πc" where ω is angular frequency and c is the light speed in the vacuum. According to this figure, the maximum band gap will be obtained for r/a=0.2. Fig. 3 shows the PBG for r/a=0.2, where the horizontal axis represents the line connecting points of first Brillion zone (the smallest space in the lattice structure). According to this figure, the PBG extends from 0.365 to 0.460. The center of the PBG is a/λ=0.412, which by considering λ=1.55μm the lattice constant will be equal to 632nm.

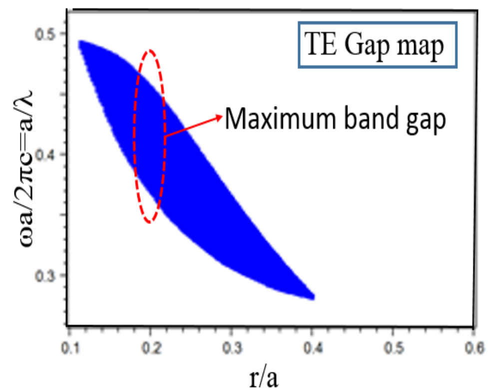

Fig. 2. Photonic crystal gap map for various radii of rods in a square lattice of As-S-Se.

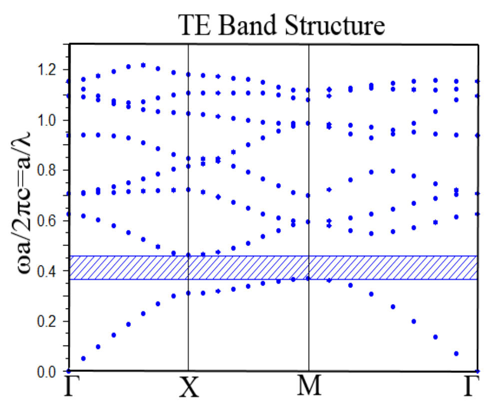

Fig. 3. (Color blue online) Band diagram in a two-dimensional square lattice rods for r/a=0.

In the next step, by using this PBG range, considering a=632nm and λ_0=1550nm (λ_0 is the central wavelength of the input light), we will design a T-shaped waveguide that includes a cavity in its path (see Fig. 4). For increasing the output of the vertical channel, we have added reflector rods at the end of the horizontal waveguide. The resonant frequency of the cavity is obtained for different values of R_1 and R_2 by exciting a pulse at the port A, and then detecting frequency response at the output (port B). Near the resonance frequency, the light from the input waveguide is coupled into the cavity and the cavity couples the light into the output waveguide, in turn. It is worth noting that the wavelength width of the input pulse should be inside the band gap of the structure, because the input light should not penetrate into other regions of the structure.

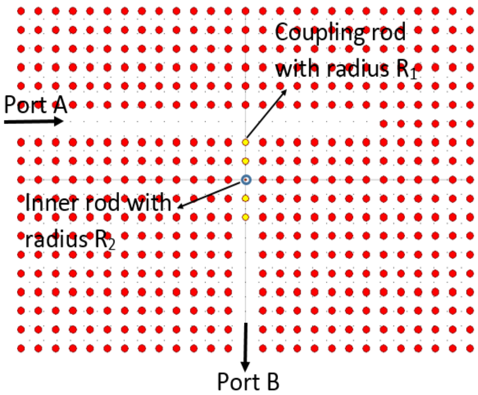

Fig. 4. The proposed T-shaped photonic crystal waveguide topology.

We use a pulse that consists of a Gaussian envelope function multiplied by a sinusoidal carrier and expressed as*:*

$$E_y(x,t)=\sqrt{P}\exp(\frac{-x^2}{W_0^2})\exp[-(\frac{t-t_0}{\tau})^2]\sin(\frac{2\pi ct}{\lambda_0})$$

Where P is the power of the excitation equal to unity, λ_0 is the central source wavelength equal to 1550 nm, w_0 is the spatial width of the pulse equal to 632 nm, τ is the pulse duration equal to 5fs and t_0 is a delay time equal to 20τ. Fig. 5 shows normalized power through a detector located in port B. Numerical values used for R_1 from 112.75 to 128.126 nm with increment 3.844 is shown in the table 1. In this case, R_2 is chosen equal to zero. Results show that the resonant wavelengths for these radii are 1.522, 1.528, 1.533, 1.540 and 1.545 micrometers respectively. It could be seen that with decreasing R_1, the resonant wavelength shifts to lower wavelengths. This is reasonable, because the resonant wavelength is proportional to the optical path passed by the light that is proportional to the circumference of the cavity. In addition, the peak values decrease which is a consequence of the larger impact of the defect on the structure of the photonic crystal. According to the Fig. 4, for separating wavelengths 1.533µm and 1.545µm, an appropriate choice is to select R_1=120.438nm and R_2=128.126nm.

Table 1. Numerical results for different values of R_1 with R_2 equal to zero.

R_1(nm)	Resonant wavelength (µm)	Value of the peak in resonant wavelength
128.126	1.545	1
124.282	1.540	0.972
120.438	1.533	0.951
116.594	1.528	0.909
112.750	1.522	0.650

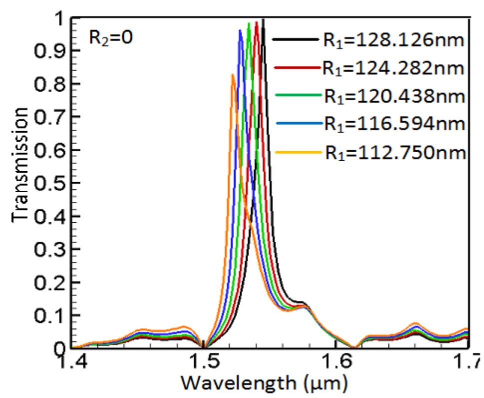

Fig. 5. Normalized power transmission spectra of the proposed T-shaped waveguide for different radii of the coupling rods R_1 with R_2 equal to zero.

In the following, for having a cavity that is able to efficiently filter wavelength 1560nm, the effect of R_2 value on the resonant wavelength of the cavity is studied. We vary the radius of the inner rod of the cavity (R_2) and keep R_1 intact. Fig. 6 shows resonant wavelengths for R_1=128.126 nm and R_2 equal to 38.43, 30.43 and 22.74 nm. The resonant wavelengths for these radii are 1.583, 1.566 and 1.557 micrometers respectively.

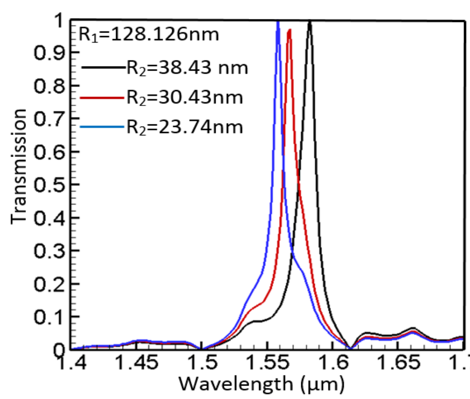

Fig. 6. Normalized power transmission spectra of the proposed T-shaped waveguide for R_1=128.126nm with different values of R_2.

The same procedure is repeated for R_1=120.438 nm. The result is shown in the Fig. 7. In this case, the resonant wavelengths for different amounts of R_2 are 1.57, 1.555 and 1.547 micrometers respectively.

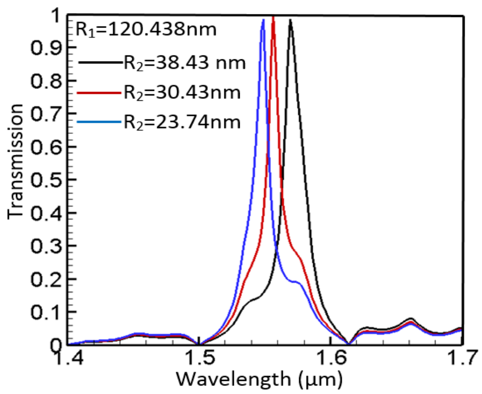

Fig. 7. Normalized power transmission spectra of the proposed T-shaped waveguide for R_1=120.438nm with different values of R_2.

Finally, for R_1=116.594 nm with different values of R_2 equal to 38.43, 30.43 and 22.74 nm, resonant wavelengths are 1.564, 1.551 and 1.541 micrometers respectively (see Fig. 8). In the summary, for separating wavelengths 1.545, 1.533 and 1.56 micrometers, a good choice is to design cavities with R_1 =128.126 with R_2 =0, R_1 =120.438 with R_2 =0 and R_1=116.594 with R_2 =38.43nm respectively.

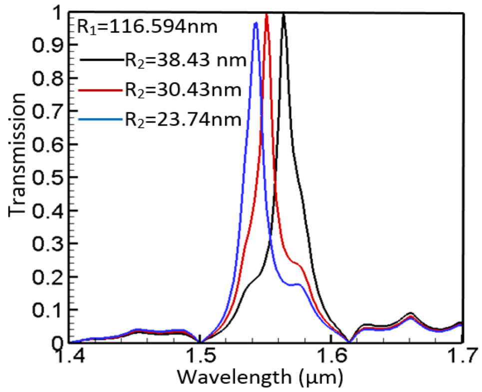

Fig. 8. Normalized power transmission spectra of the proposed T-shaped waveguide for R_1=116.594nm with different values of R_2.

Now, according to obtained results, in the following, we use three cavities to design a WDDM for filtering three wavelengths 1.533, 1.545 and 1.56 micrometers. These wavelengths are sample wavelengths, the same procedure may be repeated for every other desired set of wavelengths. The schematic design of our structure with details of the cavities is shown in Fig. 9.

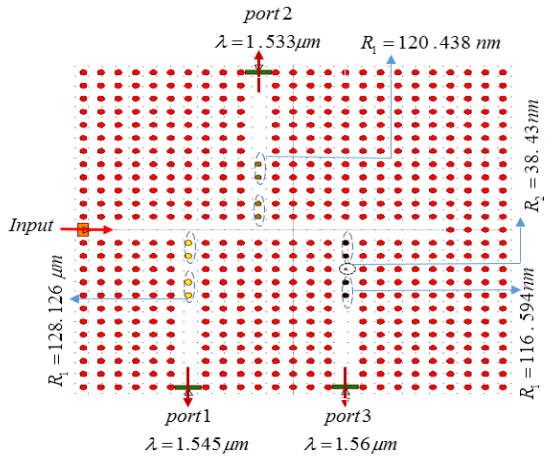

Fig. 9. Detailed design of a three channel WDDM.

Fig. 10 shows electric field pattern when a continuous wave with λ=1.545μm is lunched into the input port. As we see, almost of all the input power passes through port 1. The transmission measured along the port 1 is 99%. In other words, port 1 is ON and ports 2 and 3 are OFF.

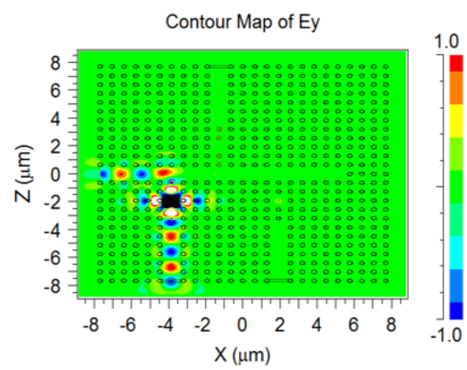

Fig. 10. Simulation pattern for λ=1.545μm.

For the λ=1.533μm source, the results of the simulation are displayed in Fig. 11. We achieve 92% transmission along output channel 2.

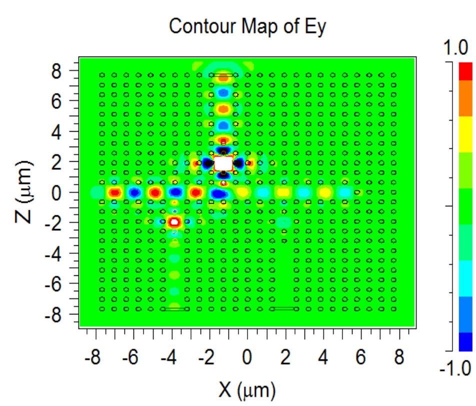

Fig. 11. Simulation pattern for λ=1.533μm.

Finally, with lunching λ=1.560µm into the input port, we observe 99% transmission along output port 3 (see Fig. 12).

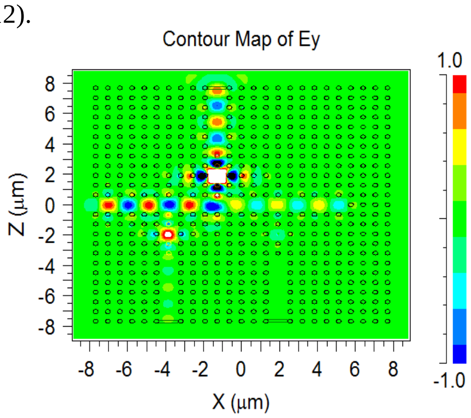

Fig. 12. Simulation pattern for λ=1.560µm.

4. CONCLUSION

In this paper, we have designed and simulated a high efficiency wavelength de-multiplexer based on a photonic crystal in a square lattice in two dimensions for separating wavelengths 1.545µm,1.545µm and 1.560µm by appropriate selections of radii of the coupling rods (R_1) and the radii of the inner rods of the cavity (R_2). The proposed structure is practical and easy-to-fabricate due to not using any complex material or structure, which is a big advantage with respect to previous complex structures used for designing WDDMs.

Results shows that the proposed WDDM has high power transmission at the output signal at the resonance frequencies and does not allow propagation of any signal for the rest of the band gap region. Obviously, the multiplexer may be redesigned to filter any other set of wavelengths.

REFERENCES

[1] E. Yablonovitch, "**Inhibited Spontaneous Emission in Solid State Physics and Electronics,**" *Physical Review Letters*, Vol. 58, pp. 2059–2062, 1987.

[2] J.D. Joannopoulos, R.D. Meade and J.N. Winn, "**Photonic Crystals Molding the Flow of Light,**" *Princeton University Press, Princeton*, NJ, USA, 1995.

[3] E. Centeno and D. Felbacq, "**Guiding Waves with Photonic Crystals,**" *Optics Communications*, Vol. 160, No. 35, pp. 57–60, 1999.

[4] T. Baba, N. Fukaya and J. Yonekura, "**Observation of Light Propagation in Photonic Crystal Optical Waveguides with Bends"** *Electronics Letters*, pp. 654–655, 1999.

[5] P.R. Villeneuve, D.S. Abrams and S. Fan, J. D. Joannopoulos, "**Single-mode Waveguide Microcavity for Fast Optical Switching Optics,**" *Letters*, pp. 2017–2019, 1996.

[6] P. R. Villeneuve, S. Fan and J. D. Joannopoulos, "**Microcavities in Photonic Crystals: Mode Symmetry, Tunability, and Coupling Efficiency,**" *Physical Review B*, Vol. 54, pp. 7837–7842, 1996.

[7] E. Centeno, B. Guizal and D. Felbacq, "**Multiplexing & Demultiplexing with Photonic Crystal,**" *J. Opt. A: Pure Appl. Opt*, 1, 1999.

[8] A. Sharkawy, S. Shi and D. W. Prather, "**Multichannel Wavelength Division Multiplexing with Photonic crystals,**" *Appl. Opt*, Vol. 40, pp. 2247-2252, 2001.

[9] M. Koshiba, "**Wavelength Division Multiplexing and Demultiplexing with Photonic Crystal Waveguide Couplers,**" *J. Lightwave Technol*, Vol. 19, pp. 1970-1975, 2001.

[10] D. Pustai, A. Sharkawy, S. Shouyuan and D. W. Prather, "**Tunable Photonic Crystal Microcavities,**" *Appl. Opt*, Vol. 41, pp. 5574-5579, 2002.

[11] S. Kim, I. Park, H. Lim and C. S. Kee, "**Highly Efficient Photonic Crystal-Based Multichannel Drop Filters of Three-Port System with Reflection Feedback,**" *Opt. Express*, pp. 5518-5525, 2004.

[12] J. Zimmermann, M. Kamp, A. Forchel and R. Marz, "**Photonic Crystal Waveguide Directional Couplers as Wavelength Selective Optical Filters,**" *Opt. Commun*, Vol. 230, pp. 387–392, 2004.

[13] Ch.Yang Liu and L.Wen Chen, "**Tunable Channel Drop Filter in a Two-Dimensional Photonic Crystal Modulated by a Nematic Liquid Crystal,**" *Journal of Nanomaterials*, pp. 1–6, 2006.

[14] K. AOKI, S. NODA and T. BABA, "**Roadmap on Photonic Crystals,**" *Kluwer Academic Publishers*, 2003.

[15] A. Taflove and S. C. Hagness, "**The Finite Difference Time Domain Method,**" *Artech House, Boston, Mass*, USA, 1998.

[16] M. Koshiba, Y. Tsuji and S. Sasaki, "**High-Performance Absorbing Boundary Conditions for Photonic Crystal Waveguide Simulations,**" *IEEE Microwave and Wireless Components Letters*, Vol. 11, pp. 152–154, 2001.